LAWRENCE
LIVERMORE
NATIONAL
LABORATORY

LLNL-TR-410827

Model-based flaw localization from perturbations in the dynamic response of complex mechanical structures

D. H. Chambers

February 25, 2009

Disclaimer

This work performed under the auspices of the U.S. Department of Energy by Lawrence Livermore National Laboratory under Contract DE-AC52-07NA27344.

FY08 LDRD Final Report

Model-based flaw localization from perturbations in the dynamic response of complex mechanical structures

LDRD Project Tracking Code: 08-ERD-063

Principal Investigator: David H. Chambers

Abstract

A new method of locating structural damage using measured differences in vibrational response and a numerical model of the undamaged structure has been presented. This method is particularly suited for complex structures with little or no symmetry. In a prior study the method successively located simulated damage from measurements of the vibrational response on two simple structures. Here we demonstrate that it can locate simulated damage in a complex structure. A numerical model of a complex structure was used to calculate the structural response before and after the introduction of a void. The method can now be considered for application to structures of programmatic interest. It could be used to monitor the structural integrity of complex mechanical structures and assemblies over their lifetimes. This would allow early detection of damage, when repair is relatively easy and inexpensive. It would also allow one to schedule maintenance based on actual damage instead of a time schedule.

1. Introduction

Structural health monitoring (SHM) is the process of implementing a strategy for detecting and identifying damage in a structure or machine.[1] Damage is a change in the material and/or geometrical properties of a structural that adversely affects its performance. It could be a local change in material properties, a loss of connectivity between components, or a change in boundary conditions. The SHM process generally involves periodic observation of a structure or mechanical system, extraction of damage-sensitive features from the measurements, and an analysis of the features to identify specific types of damage[1]. This is often followed by an assessment of expected future performance and probability of failure.

SHM is motivated by the need within both industry and government to detect damage as early as possible. Early detection makes repair easier, minimizing cost and economic impact, as well as reducing the risk of failure and possible loss of life. In addition, there are potential cost savings in moving from the current time-based maintenance approach to condition-based approaches using SHM. Current implementations of SHM include conditional monitoring (CM) of rotating and reciprocating machinery[1], and the Shuttle Modal Inspection System (SMIS) for locating damaged components covered by the thermal protection tiles on the space shuttle[2,3]. Active research is currently underway for developing SHM systems for civil infrastructure (bridges, highways), monitoring of composite materials in aircraft, and assessing structural integrity of buildings (see reviews by Doebling[2] and Farrar[1]). With the further development of smart sensors and nanotechnology, SHM techniques will likely be incorporated directly into the design of structures and critical mechanisms.

The predominant physical mechanism used for SHM is vibration, or the dynamic response, of the mechanical system. Since vibration (and more generally acoustics) depends directly on the material properties and geometrical integrity of the system, it is the most direct mechanism for assessing structural health[2]. It has long been known that local changes in material stiffness, mass, or geometry create measurable changes in the dynamic response of a structure. For practical reasons, the number of sensors is typically much less than the number of structural components. Thus most of the work in SHM has concentrated on using the low vibrational frequencies in which the entire structure takes part in the motion. This makes it difficult to solve the important *inverse problem*, in which damage is located and characterized from a limited number of vibration measurements[4]. Higher vibration frequencies would be more sensitive to the local structural changes induced by damage. However, these are more difficult to analyze since their characteristics are more sensitive to material inhomogeneities, dissipation, and uncertainties in the numerical models typically used to solve the inverse problem.

Recently, a new set of techniques based on the invariance of wave propagation to time reversal has been used for source localization, imaging, and ultrasonic nondestructive evaluation [5,6,7]. These have been applied to imaging of a mass bonded onto an aluminum plate using Rayleigh-Lamb waves[8].

In each of these studies the time-reversal imaging was obtained either by simulation or by measuring the entire wave field in geometries where the interior of the object was accessible. In this paper, we describe a time-reversal technique for detecting and localizing damage in the usually inaccessible interior of a structure. The technique is implemented in the context of structural health monitoring, where the appearance of damage causes a detectible change in the vibrational response. After a brief theoretical justification of the method, we describe the initial proof-of-concept experiments for simple shapes. Finally, we show the numerically simulated results for a complex object.

2. Localization method: theory

In structural health monitoring, a set of sensors would be emplaced in the structure and the vibrational response checked periodically. A change in response would indicate the presence of damage, typically localized when detected early. Though structural vibration is described by the equations of linear elasticity, we will present the theory for the acoustic case. The generalization to elastic structures is straightforward.

Let $\psi(\mathbf{x})$ represent the acoustic (vibrational) field within an object at a given frequency ω. The field is described by the Helmholtz equation

$$\nabla^2\psi + k_0^2 U(\mathbf{x})\psi = s(\mathbf{x}), \tag{1}$$

where k_0 is a wave number characteristic of the structure. The function $s(\mathbf{x})$ represents the sources of waves. The *potential function* $U(\mathbf{x})$ specifies the variations from the background wave number that describe the internal structure of the object. The governing equation is supplemented by boundary and initial conditions that together uniquely specify the acoustic field. Let $U_0(\mathbf{x})$ describe the initial structural configuration of the object, and $\delta U(\mathbf{x})$ the deviations from the initial configuration caused by structural damage. The change $\delta\psi$ in the acoustic field caused by the presence of damage is described by the equation

$$\nabla^2\delta\psi + k_0^2 U_0(\mathbf{x})\delta\psi = s_{eff}(\mathbf{x}), \tag{2}$$

where s_{eff} is an *effective* source given by

$$s_{eff}(\mathbf{x}) = -k_0^2 \left(\psi_0(\mathbf{x}) + \delta\psi(\mathbf{x})\right) \delta U(\mathbf{x}). \tag{3}$$

The quantity ψ_0 is the acoustic field for the undamaged configuration. Ideally for damage characterization, we would like to estimate the change in potential δU from a set of discrete measurements of the perturbed acoustic field. The presence of the perturbed field $\delta\psi$ in the expression for the effective source (eq. 3) makes this inverse problem nonlinear. It is a difficult ill-posed problem that is usually solved using an iterative algorithm that involves guessing an initial solution, calculating the expected perturbed field, comparing with the measured data, then updating the solution[4]. This is repeated until the solution converges or the deviations from the data decrease below a predetermined threshold. The solution of the inverse problem is an area of active research. However, it is often valuable to know just the location of the damaged region, especially when this knowledge is supplemented by other indications of damage (e.g. chemical breakdown products).

The effective source s_{eff} in the equation for the perturbed acoustic field $\delta\psi$ is proportional to the perturbed potential δU. Structural damage (represented by δU) in its early stage is often localized to a small region in the structure. The damage acts like a localized source for the perturbed acoustic field. In addition, the propagation of the perturbed field is governed by the initial unperturbed configuration (U_0 in eq. 2). Thus the localization problem is: given a discrete set of measurements of an acoustic field on the external surface of a structure, estimate the region of support for the internal source distribution that generates the field in the initial configuration of the structure. We will calculate an approximate solution to this problem using a numerical model of the structure in its known undamaged state. It proceeds in four steps: 1) measure the dynamic response of a structure at a discrete set of locations before and after damage, 2) subtract the responses to calculate the perturbed field at each location, 3) time-reverse the perturbed field values at each location and numerically propagate them into a model of the undamaged structure, 4) identify the source location with the peak in the time-reversed field. More formally, if $\delta\psi_n$ are the values of the perturbed field at $\mathbf{x}_n$ $n = 1, 2, ..., N$, we calculate the backpropagated field

$$\chi(\mathbf{x}) = \sum_{n=1}^{N} \psi_n^* G_0(\mathbf{x}; \mathbf{x}_n), \tag{4}$$

where $G_0(\mathbf{x}; \mathbf{x}_n)$ is the Green's function,

$$\left(\nabla^2 + k_0^2 U_0(\mathbf{x})\right) G(\mathbf{x}; \mathbf{x_n}) = -\delta(\mathbf{x} - \mathbf{x}_n). \tag{5}$$

The backpropagated field can be interpreted as an acoustic field but it is more useful to regard it as a detection map, similar to the ambiguity function of matched field processing[9]. The maxima in the field are probable locations of damage that create an effective source for the measured perturbed field.

Though we have presented the theory of the method for a single frequency, it remains valid for broadband excitations. The remarkable ability of time-reversal arrays in focusing energy back to a source is well known (see review by Fink[6]). This focusing effect is enhanced for difficult or random media[10,11,12,13,14]. In our approach to damage detection, we make use of the time-reversal focusing property in the numerical backpropagation. We can then expect the performance of the method to be particularly good for complicated structures with little or no symmetry. However, our initial tests used symmetrical objects because of the wide range of structures that incorporate components with these shapes.

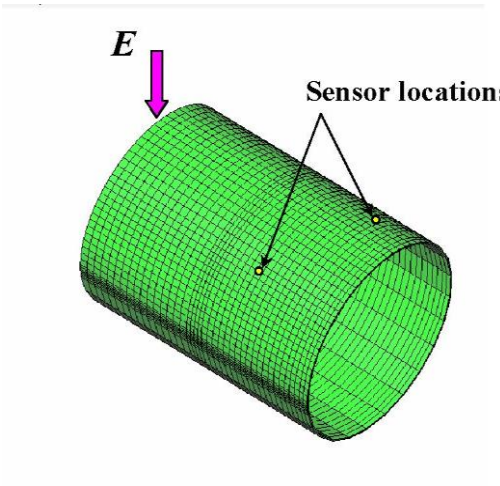

Figure 1. Numerical model of aluminum cylinder for damage detection experiment. E indicates the postion of the forcing. The yellow dots show the positions of the Fiber-Bragg strain sensors.

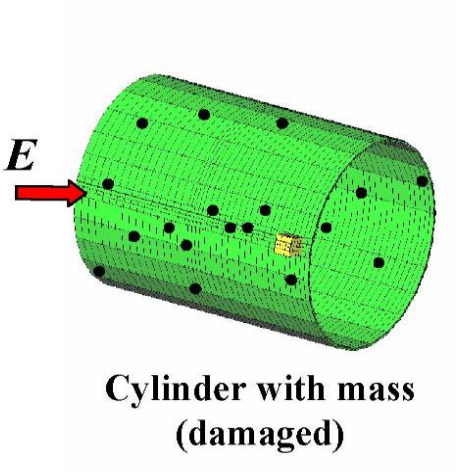

Figure 2. Numerical model of aluminum cylinder for damage detection experiment showing small cube attached at one end to simulate damage. E indicates the position of the forcing. The black dots show the positions of the 20 simulated sensors in a numerically simulated experiment.

3. Performance for simple objects

The first test of the damage detection method used a thin-walled (3 mm thick) aluminum cylinder (212 mm diameter). Two Fiber-Bragg optical strain sensors were attached to the outer wall of the cylinder (Fig. 5). The vibrational response was measured as a time-dependent force was applied at one end. The forcing function was a swept sine wave from 1 kHz to 5 kHz. After the response was recorded, a small cubic mass of aluminum (40 gm) was attached near the edge of the cylinder opposite the forcing (Fig. 1). The differences between the responses at each sensor location were time-reversed and applied as normal forces in a numerical simulation of original cylinder. The magnitude of the resulting displacement field in the numerical model is shown in Fig. 4. This can be compared with the results from a numerical simulation of an experiment using 20 sensors (Fig. 3). We see a maximum in the displacement magnitude near the location of the added mass. There is a remarkable agreement between the numerically simulated experiment with 20 sensors and the actual experimental data with two sensors. In both cases there are secondary maxima (one associated with the forcing point) due to the symmetry of the cylinder.

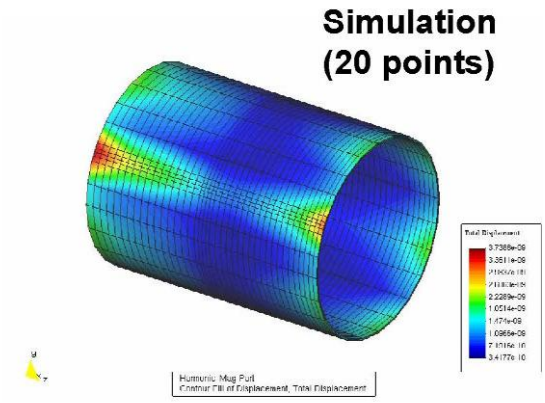

Figure 3. Magnitude of the numerically simulated displacement field obtained by backpropagating the differences between the simulated displacements at the 20 locations in Fig. 1

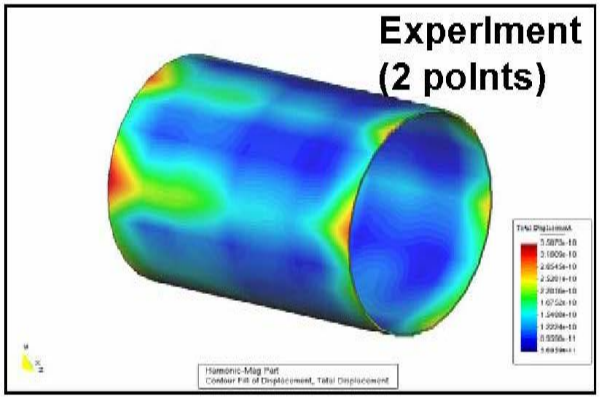

Figure 4. Magnitude of the numerically simulated displacement field obtained by backpropagating the differences between the strains measured by the two Fiber-Bragg sensors. Local maxima can be seen at the positions of the forcing and the added mass.

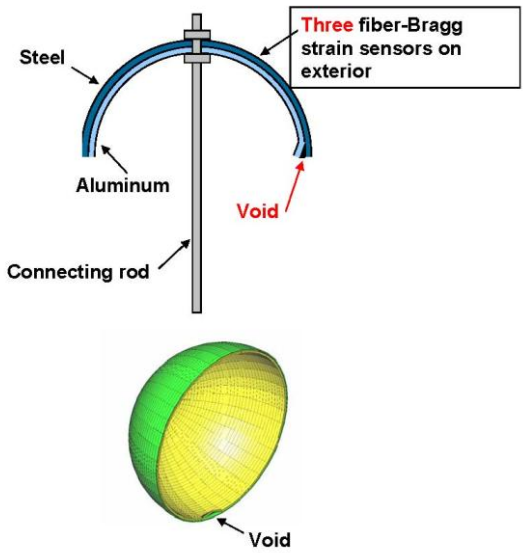

Figure 5. Diagram of the two nested hemispheres (top) for the second test of the damage detection method. Lower figure shows a numerical model of the hemispheres with a localized bend in the inner sphere to model a void.

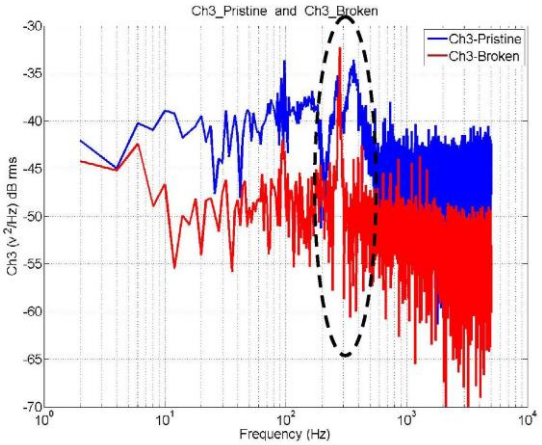

Figure 6. Power spectra of one of three Fiber-Bragg sensors before (blue) and after (red) bending of the lipo of the inner hemisphere. The main difference between spectra is the presence of the peak for the bent configuration (black oval) near 2600 Hz.

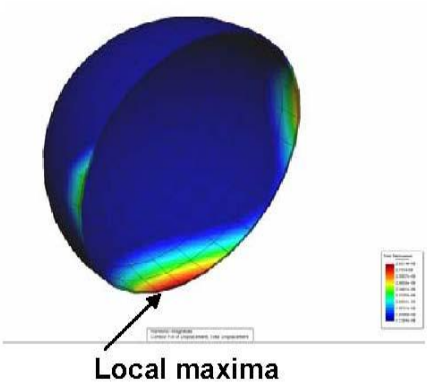

Figure 7. Magnitude of the displacement for the backpropagated field for the nested spheres. A maximum occurs at the location of the bent region (damage)

The second test used a pair of nested hemispheres held together by a rod at the poles (Fig. 5). The outer hemisphere was composed of steel and the inner hemisphere composed of aluminum. Three Fiber-Bragg strain sensors were attached to the surface of the outer hemisphere. A small void at the position of the lip was created by bending a section of the inner hemisphere inward. The vibrational responses before and after bending were recorded by the three strain sensors. Figure 6 shows the power spectra from one sensor for the original and bent configurations. The main difference is a large peak near 2600 Hz in the spectrum of the bent configuration. If the response at this frequency is time-reversed and applied as a normal force in a numerical model of the hemispheres, a maximum is seen in a map of the displacement magnitude (Fig. 7) at the location of the bend.

These initial experimental tests of the damage localization method were part of an earlier feasibility study. They showed that the method was robust to measurement noise and other uncertainties inherent in experimental measurement for simple objects. The method had never been applied to a complex structure typical of most applications of interest. As a preliminary investigation of this issue, the current project tested the backpropagation method for damage localization on a numerical simulation of a complex structure. The specific numerical structural model is shown in Fig. 8. It consists of a sphere nested between several disks and composed of five different materials. The normal displacement at 18 locations on one end were calculated when an impulse was applied at one point. The model was then modified by reducing the density and elastic modulus of four small elements in the lexan to 1% and 0.1%, respectively, of their original values. This simulated the presence of a small void in the Lexan. Figure 9 shows the displacements at the 18 locations before and after modifying the four elements in the Lexan. It also shows the time-reversed difference used as the normal forcing at the 18 locations for the simulation of the backpropagated field. Figure 10 shows the magnitude of the axial strain of the backpropagated field. The maximum of the strain field occurs at the position of the void. Additional tests on two other complex structures showed similar results. These results establish that the backpropagation method of damage location applies in principle to complex objects. The method can now be considered for specific applications of programmatic interest.

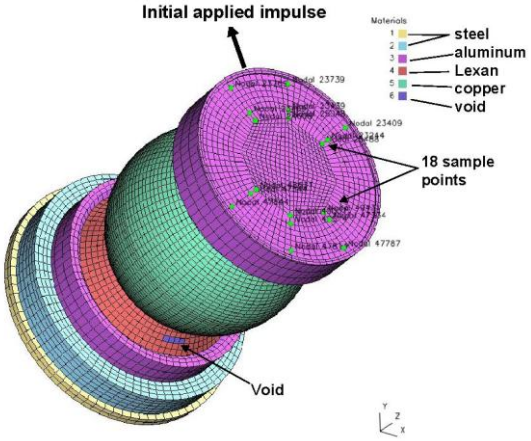

Figure 8. Numerical model of a sphere between disks used for calculating the normal displacement at 18 sample locations in response to an impulse applied at the upper end. The responses were calculated for the original configuration without the void and for the void configuration.

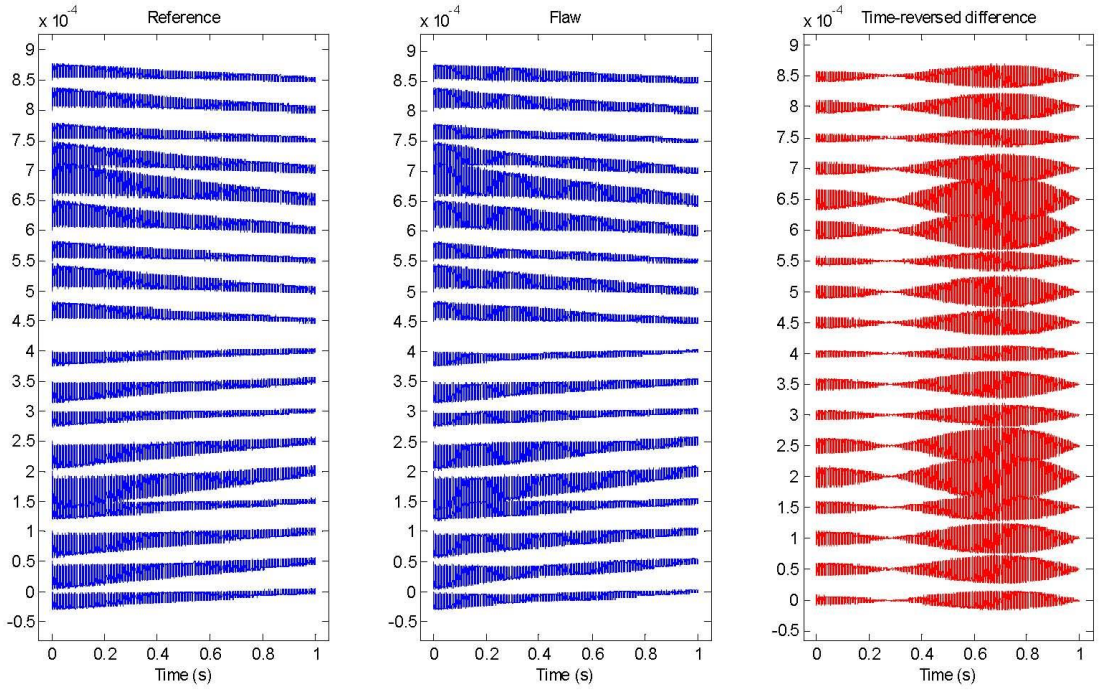

Figure 9. Normal displacements at the 18 sample locations in Fig. 8 for the original (left) and void configuration (center). The time-reversed normal forces for the backpropagation step are shown on the right.

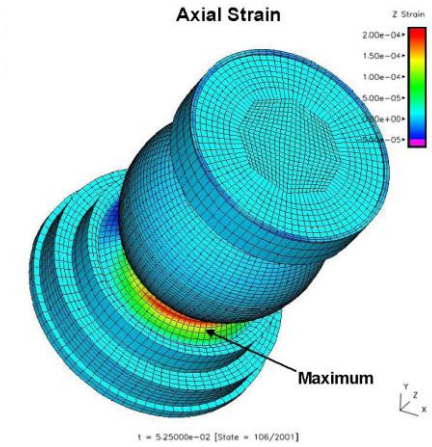

Figure 10. Magnitude of the axial strain for the backpropagated field in the numerical model of a sphere between disks. A maximum is clearly seen at the position of the simulated void.

4. Summary

A new method of locating structural damage using measured differences in vibrational response and a numerical model of the undamaged structure has been presented. This method is particularly suited for complex structures with little or no symmetry. In a prior study the method successively located simulated damage from measurements of the vibrational response on two simple structures. Here we demonstrate that it can locate simulated damage in a complex structure. A numerical model of a complex structure was used to calculate the structural response before and after the introduction of a void. The method can now be considered for application to structures of programmatic interest. It could be used to monitor the structural integrity of complex mechanical structures and assemblies over their lifetimes. This would allow early detection of damage, when repair is relatively easy and inexpensive. It would also allow one to schedule maintenance based on actual damage instead of a time schedule.

5. Acknowledgements

The Principal Investigator would like to acknowledge the work of his co-investigators Henry Hsieh, Karl Fisher, Lisle Hagler, and Sean Lehman.

This document was prepared as an account of work sponsored by an agency of the United States government. Neither the United States government nor Lawrence Livermore National Security, LLC, nor any of their employees makes any warranty, expressed or implied, or assumes any legal liability or responsibility for the accuracy, completeness, or usefulness of any information, apparatus, product, or process disclosed, or represents that its use would not infringe privately owned rights. Reference herein to any specific commercial product, process, or service by trade name, trademark, manufacturer, or otherwise does not necessarily constitute or imply its endorsement, recommendation, or favoring by the United States government or Lawrence Livermore National Security, LLC. The views and opinions of authors expressed herein do not necessarily state or reflect those of the United States government or Lawrence Livermore National Security, LLC, and shall not be used for advertising or product endorsement purposes.

This work performed under the auspices of the U.S. Department of Energy by

Lawrence Livermore National Laboratory under Contract DE-AC52-07NA27344. This work was funded by the Laboratory Directed Research and Development Program at LLNL under project tracking code 08-ERD-063.

References

[1] C. R. Farrar and K. Worden. An introduction to structural health monitoring. *Phil. Trans. Royal Soc. A*, 365:303–315, 2007.
[2] S. W. Doebling, C. R. Farrar, and M. B. Prime. A summary review of vibration-based damage identification methods. *The Shock and Vibration Digest*, 30:91–105, 1998.
[3] D. L. Hunt, S. P. Weiss, W. M. West, T. A. Dunlap, and S. R. Freemeyer. Development and implementation of a shuttle modal inspection system. *Sound and Vibration*, 24:34–42, 1990.
[4] M. I. Friswell. Damage identification using inverse methods. *Phil. Trans. Royal Soc. A*, 365:393–410, 2007.
[5] E. Kerbrat, C. Prada, D. Cassereau, and M. Fink. Ultrasonic nondestructive testing of scattering media using the decomposition of the time-reversal operator. *IEEE Trans. Ultrason., Ferroelect., Freq. Contr.*, 49:1103–1113, 2002.
[6] M. Fink, D. Cassereau, A. Derode, C. Prada, P. Roux, M. Tanter, J.-L. Thomas, and F. Wu. Time-reversed acoustics. *Rep. Prog. Phys.*, 63:1933–1995, 2000.
[7] M. Fink and C. Prada. Acoustic time-reversal mirrors. *Inverse Problems*, 17:R1–R38, 2001.
[8] C. H. Wang, J. T. Rose, and F-K. Chang. A synthetic time-reversal imaging method for structural health monitoring. *Smart Mater. Struct.*, 13:415–423, 2004.
[9] A. Tolstoy. *Matched Field Processing for Underwater Acoustics*. World Scientific, Singapore, 1993.
[10] L. Borcea, G. C. Papanicolaou, C. Tsogka, and J. G. Berryman. Imaging and time reversal in random media. *Inverse Problems*, 18:1247–1279, 2002.
[11] J. G. Berryman, L. Borcea, G. C. Papanicolaou, and C. Tsogka. Statistically stable ultrasonic imaging in random media. *J. Acoust. Soc. Am.*, 112:1509–1522, 2002.
[12] P. Blomgren, G. Papanicolaou, and H. Zhao. Super-resolution in time-reversal acoustics. *J. Acoust. Soc. Am.*, 111:238–248, 2002.
[13] A. Derode, A. Tourin, and M. Fink. Random multiple scattering of ultrasound. i. coherent and ballistic waves. *Phys. Rev. E*, 64:036605–1–036605–7, 2001.
[14] A. Derode, A. Tourin, and M. Fink. Random multiple scattering of ultrasound. ii. is time revesal a self-averaging process? *Phys. Rev. E*, 64:036606–1–036606–13, 2001.